Screech Characterization using POD and DMD Analysis

A Nageswara Rao, Abhijit Kushari*, Alakesh Chandra Mandal

Department of Aerospace Engineering, Indian Institute of Technology Kanpur, UP, India
*corresponding author: akushari@iitk.ac.in

Abstract
The present study investigates the acoustic characteristics of a jet emanating from a high Aspect ratio convergent elliptic nozzle at under-expanded condition. Time-resolved schlieren images were acquired at exit Mach number 1.69. Proper orthogonal decomposition (POD) and Dynamic mode decomposition (DMD) techniques were performed on the time-resolved schlieren images to identify the acoustic feedback phenomena along with the dominant flow structures. Near field acoustic measurements were conducted inside an anechoic chamber using a microphone. First 6 dominant POD modes reveal the presence of acoustic feedback phenomena. The first spatial DMD mode corresponds to the screech, and the associated frequency is found to be 10 kHz.

Keywords: Screech, Nozzle pressure ratio (NPR), Mach number, Proper Orthogonal Decomposition (POD), Dynamic Mode Decomposition (DMD).

1 Introduction

Environmental noise compliance is an increasingly stringent requirement arising from the growing impact of aviation. Under-expanded supersonic jets exhausting from convergent nozzles, used in aircraft and rockets, generate different types of noise including screech tones, shock associated noise and turbulent mixing noise with screech tones being the most dominant component in the frequency spectrum at higher Mach numbers. Screech is a self-sustained acoustic feedback loop mechanism. The interactions of large organized structures in the shear layer with the shock cell generate screech tone. The generated screech tones propagate upstream through the series of shock cells and perturb the shear layer; thus, reinforces the eddy strength at the exit of the nozzle. This perturbed structures convects downstream and interacts with the shock cell to generate the screech tones and closes the loop [1]. The most dynamic discrete sound propagates to the upstream while the first harmonic of that propagates perpendicular to the jet direction [2]. Many researchers have reported that the screech tones can cause sonic fatigue failure of aircraft structures due to high dynamic loads [3][4]. To suppress the screech sound generated from the supersonic jets, it is essential to understand the mechanism of screech and the associated flow structures. Mixing characteristics of the jets are enhanced when the elliptic geometry is used at the exit of the nozzle at subsonic and supersonic conditions. Elliptic nozzles are better mixing promoters compared to the traditional circular nozzles [5]. Many researchers have reported that for supersonic jets the noise reduction in elliptic nozzles is more compared to the circular nozzles [6] [7]. The present study aims to understand the screech generation process from the high Aspect ratio elliptic nozzle based on the POD (Proper Orthogonal Decomposition) and DMD (Dynamic Mode Decomposition) analysis. POD and DMD analysis performed on the set of time-resolved high-speed schlieren images to identify the dominant flow structures. In addition to this, microphone measurements conducted inside an anechoic chamber to corroborate the POD and DMD results.

Experimental Facility and Instrumentation:

The experiments are conducted inside an anechoic chamber designed using the conventional quarter wavelength rule and. Sound absorbing material is used on the exposed instruments as well to avoid any reflections. The inner dimensions of the anechoic chamber are 4.2 x 4.1 x 2 m with the cut-off frequency of 400 Hz. The schematic of the anechoic chamber with an open jet facility is shown in Fig. 1. This test facility consists of an anechoic chamber, a pressure regulating valve, a venturi meter and the settling chamber with a collar pipe. The nozzle is fitted to the collar pipe using a flange. The settling chamber pressure is the driving parameter of the present work, and it is maintained constant throughout the test using a pressure regulating valve. The stagnation pressure (P_{01}) is measured through a pressure tap over the settling chamber (SC). The settling chamber pressure is changed according to the desired nozzle pressure ratio (NPR). The standard definition for the nozzle pressure ratio is the stagnation pressure (P_{01}) to the ambient pressure (P_{amb}). Near field microphone measurements are carried out for the elliptic nozzle at NPR 4. A microphone is located upstream of the nozzle as shown in Fig. 6. The intent of placing the microphone at this location is to capture the acoustic feed-back waves that are propagating upstream of the jet and avoid the remaining noise components such as turbulent mixing noise.

The present experimental investigation is carried out on a convergent elliptic nozzle with Aspect ratio 7:1. The isometric view of the nozzle CAD model is also shown in Fig.1. The experiments are conducted for the jet Reynolds number of 3.1 x 10^5, which corresponds to the Nozzle pressure ratio (NPR) of 4. Reynolds number is estimated based on the nozzle exit conditions and exit hydraulic diameter (D_h).

Z-type schlieren visualization technique is used to capture the jet field along with the acoustic waves. The schematic of the schlieren setup is illustrated in Fig.1. The schlieren setup consists of an LED light source, concave mirrors, a knife-edge and a high-speed camera to capture the images. The light ray from the light source passes through the iris and strikes the first concave mirror. The LED light is kept at the focal point of the first concave mirror and thus the diffused beam becomes collimated after striking it. This beam passes through the jet flow field area to strike second concave mirror. Finally, the reflected ray from the second mirror passes through a knife edge at its focal point and falls on the camera lens. When the beam passes through the supersonic jet field light rays get deflected due to the refractive index gradient (n'). This gradient is directly proportional to the flow density gradient. The images are acquired at a rate of 41,000 fps and the exposure time is kept at 7μs so that the feedback phenomena along with the shear layer interaction can be captured.

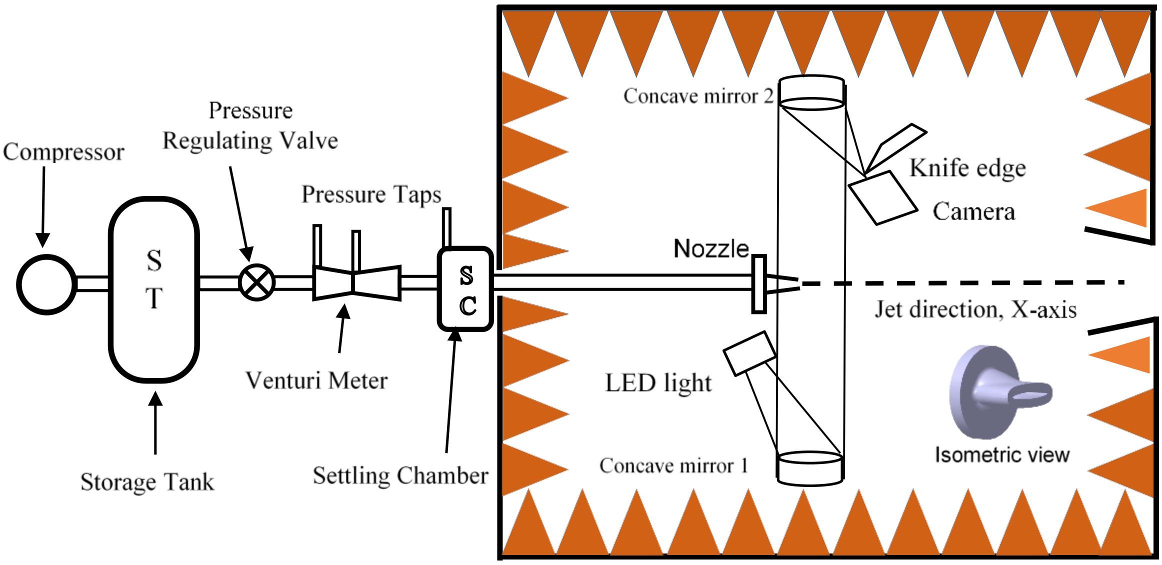

Figure 1. Anechoic chamber with open jet test facility.

Results and Discussion:

POD Analysis on the time resolved schlieren data set:

Proper orthogonal decomposition (POD) method was initially pioneered by Kosambi [8]. The POD technique was later introduced to the turbulent community by Lumely [9]. Analyzing turbulence flow field is difficult due to its chaotic nature. Proper orthogonal decomposition is a mathematical technique which reduces the system to lower dimensions based on the energy distribution across the modes. POD determines the optimal basis functions by identifying the dominant structures with the largest mean square projection of the system using a two-point spatial correlation tensor in an eigenvalue problem. POD technique was later modified as a method of snapshots by Sirovich [10]. In this technique, 'n' number of snapshots of the flow field is captured with an equal time interval of Δt. Then, this spatiotemporal field is divided into time-dependent coefficients and spatial basis functions. The complete mathematical description of the POD technique is briefly discussed in the literature [9] [10] [11]. In the present investigation, snapshot POD is done on time-resolved scalar schlieren data. The refractive index gradient (n') is considered as the scalar field for the current analysis.

To quantify the screech phenomena an experimental investigation is carried out on an elliptic jet at under expanded condition, NPR 4. As mentioned earlier, schlieren snapshots are captured using a high-speed camera at a rate of 41,000 fps with the exposure time 7μs. Figure 2 shows an instantaneous schlieren image for the elliptic jet at NPR 4. Schlieren image illustrates that strong shock cells are forming downstream of the nozzle exit. It is also observed that a series of acoustic waves are propagating from the location where the shock cells appear to collapse, which are known as screech tones [1]. Although the under-expanded jets emanating from the convergent nozzles generate screech tones, broadband shock associated noise and turbulent mixing noise, the current analysis focuses only on determining the characteristics of the screech tones. If the POD is performed on the current schlieren data, it is expected that the first few high energy modes would be associated with the shocks. Thus, the time mean of all snapshots are taken, and then the mean mode is subtracted from the instantaneous snapshots to get the fluctuating component of the flow field. Figure 3 shows the first image after the mean mode is subtracted. It can be observed that the unsteady components of the jet are isolated from the mean shock cell mode. However, the remaining fluctuating components such as a shear layer, acoustic waves, and turbulent structures are still present. Similarly, this mean mode is subtracted from all the schlieren snapshots, and proper orthogonal decomposition is executed on the remaining data, and then, most energetic modes are extracted.

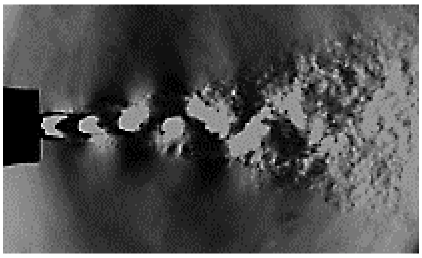

Figure 2. Instantaneous schlieren image for the elliptic jet at NPR 4.

Figure 3. First image after mean mode is subtracted.

Figure 4 shows the most dominating first 6 POD high energy modes in reducing order. Modes 1 - 6 exhibits that an acoustic wave propagating upstream which is typically known as screech tones [1]. Similar acoustic propagation was reported by Berry et al. [12] on a single expansion ramp nozzle using POD analysis on the schlieren images. Modes 1 and 2 depict the flapping of the jet about its axis along with the acoustic wave propagation. It is observed that this flapping is asymmetric for modes 1 - 3, as shown in Fig. 4. The power spectral density (PSD) of the time-dependent coefficients is presented in Fig. 5. The fundamental dominant frequency is observed at ~ 10 kHz for the modes 1-3. However, the first harmonic of the fundamental frequency is observed for mode 4. The fundamental frequency for the mode - 6 is observed to be greater than the > 10 kHz. Near field, microphone measurement was performed, and sound pressure level (SPL) spectra are presented in Fig. 6. SPL spectra show the dominant discrete fundamental frequency at ~ 10 kHz. This spectral content is observed to be similar to the POD modes 1 -3 as shown in Fig. 5. The first harmonic of the fundamental frequency is observed to be matching with mode 4 and 5. Hence, near field microphone measurements and POD analysis on the schlieren images suggests that the acoustic wave propagating upstream is the screech tone and the corresponding frequency is ~ 10 kHz.

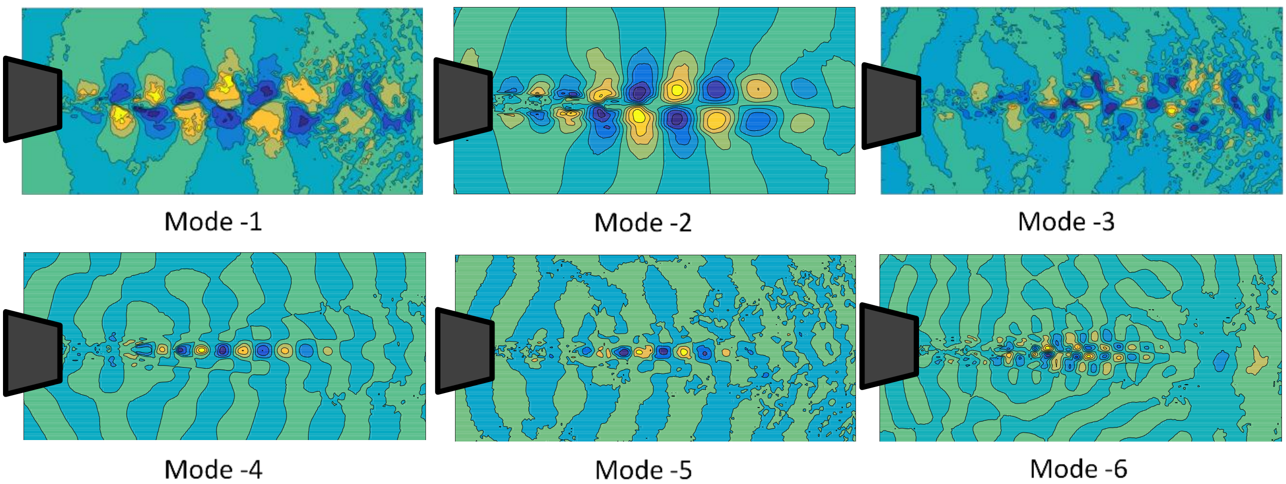

Figure 4. First 6 POD spatial eigenfunctions.

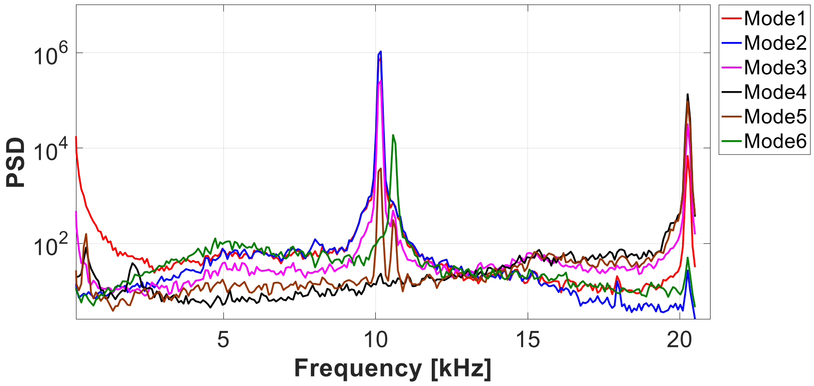

Figure 5. PSD of first 6 time dependent POD coefficients.

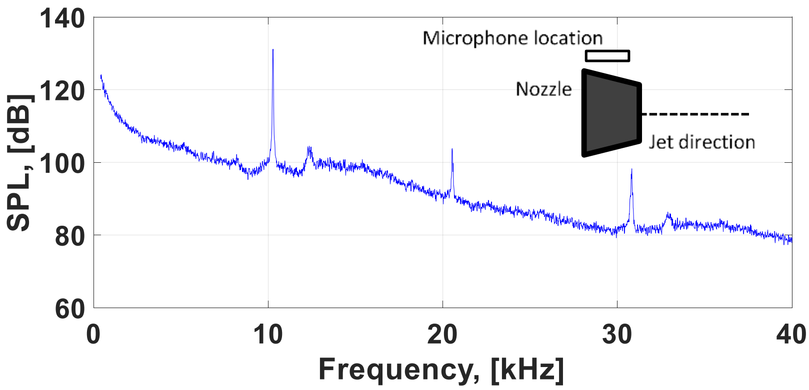

Figure 6. SPL spectra for elliptic nozzle at NPR 4.

DMD Analysis on the time resolved schlieren data set:

Dynamic mode decomposition (DMD) is a mathematical technique to extract the underlying dynamic information using time-resolved snapshots of any experimental data. Dynamic mode decomposition is closely related to the Arnoldi algorithm [13]. The temporal DMD algorithm used in the present work is adapted from Schmid [14]. The mathematical explanation for Dynamic Mode Decomposition can be found in the literature [13] [14]. The representation of fluid flow in proper orthogonal decomposition is based on the energy modes. Each energy mode consists of multiple frequencies due to the enforced orthogonality in space. However, Dynamic mode decomposition identifies the structure and sorts based on pure frequency, thus maintains orthogonality in time.

Figure 7 shows the dominant spatial structures of the dynamic mode decomposition (DMD). Figure 7 (a) represents the spatial DMD mode of acoustic feedback loop which corresponds to the fundamental frequency of 10.1 kHz. The self-sustained acoustic wave (screech tone) is observed to be originating from the third shock cell. The acoustic wave direction is observed to be spreading in both upstream and downstream directions. However, the dominant structures are observed upstream near the nozzle as seen in Fig. 7 (a). The first spatial DMD mode is closely related to the first 3 high energy POD modes. The dominant frequency of these POD modes are at 10.1 kHz which is similar to the first spatial DMD mode. Nevertheless, these POD modes consist of other jet structures like flapping and turbulence whereas DMD mode isolates the screech tones from the remaining jet structure and characterizes the acoustic feedback system in an enhanced way. Figure 7 (b) shows the second spatial mode which is similar to the 6th POD mode. This mode represents the second fundamental frequency at 10. 6 kHz which may be attributable to the screech staging phenomena. Figure 7 (c) shows the third spatial DMD mode which corresponds to the first harmonic of the fundamental frequency.

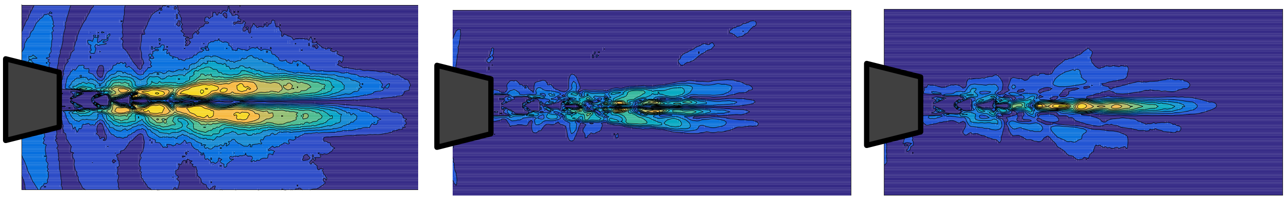

Figure 7. Dominant spatial DMD modes.

Conclusions:

The main objective of this work was to understand the acoustic characteristics from the high Aspect ratio convergent elliptic nozzle at the high under expanded condition. Proper orthogonal decomposition (POD) and Dynamic Mode Decomposition (DMD) techniques were applied on the time-resolved schlieren measurements to identify the dominant jet structures. The POD analysis reveals that jet flapping along with the acoustic waves from the first 3 dominant energy modes. The time-dependent coefficients show the dominant frequency of these corresponding modes to be ~ 10 kHz. Near field acoustic measurements were conducted and SPL spectra also verify the dominant fundamental frequency at ~ 10 kHz. The first spatial DMD mode captures the acoustic waves correspond to the screech. It is evident that the DMD modes were able to isolate the screech tones based on the frequencies.

References

[1] Powell A (1953) On the noise emanating from a two-dimensional jet above the critical pressure. *The Aeronautical Quarterly*, Vol. 4, No. 2, pp. 103-122. doi: 10.1017/S0001925900000822.

[2]. Powell Alan (1953) on the mechanism of choked jet noise. *Proceedings of the Physical Society*. Section B 66, no. 12, pp. 1039.

[3] Hay J A, and Rose E G (1970) In-flight shock cell noise. *Journal of Sound Vibration*, vol. 11, pp. 411. doi: 10.1016/S0022-460X (70)80003-7.

[4] Berndt D E (1984) Dynamic pressure fluctuations in the inter nozzle region of a twin-jet nacelle. *SAE Technical Paper*, No. 841540. doi: 10.4271/841540.

[5] Gutmark E, Schadow K C and Wilson K J(1989) Non Circular Jet dynamics in Supersonic Combustion, *Journal of Propulsion*, Vol. 5, No. 5, pp. 529-533. doi :10.2514/3.23186.

[6] Seiner John M and Michael K Ponton (1992) Supersonic acoustic source mechanisms for free jets of various geometries, *In In AGARD, Combat Aircraft Noise*, 12 p (SEE N93-10666 01-71).

[7] Kinzie K and D K McLaughlin (1995) Noise Radiated From Asymmetric Supersonic Jets, *DGLR BERICHT*, pp. 81-81.

[8] Kosambi, D D (1943) Statistics in function space, *Journal of the Indian Mathematical Society*, pp. 76-88. ISSN 0019-5839.

[9] Lumley J L (1967) The structure of inhomogeneous turbulent flows. *Atmospheric turbulence and radio wave propagation*, pp. 166-178.

[10] Lawrence S (1987) Turbulence and the dynamics of coherent structures (Part I: Coherent structures), *Quarterly of applied mathematics*, vol. 45, pp.561-571.

[11] Berry M G, Magstadt, A S and Glauser M N (2017) Application of POD on time-resolved schlieren in supersonic multi-stream rectangular jets, *Physics of Fluids*, vol. 29, no. 2, pp. 020706.

[12] Berry M G, Magstadt, A S and Glauser M N (2017) DMD and POD of time-resolved schlieren on a multi-stream single expansion ramp nozzle, *International Journal of Heat and Fluid Flow*, vol. 66, pp.60-69.

[13] Rowley CW, Mezić I, Bagheri S, Schlatter P and Henningson D S (2009) Spectral analysis of nonlinear flows, *Journal of fluid mechanics*, 641, pp.115-127.

[14] Schmid P J (2010) Dynamic mode decomposition of numerical and experimental data. *Journal of fluid mechanics*, vol. 656, pp.5-28.